Bulletin of Mathematical Biology (2010) 72: 2161–2179
DOI 10.1007/s11538-010-9533-4

ORIGINAL ARTICLE

Aberrant Behaviours of Reaction Diffusion Self-organisation Models on Growing Domains in the Presence of Gene Expression Time Delays

S. Seirin Lee[a,*], E.A. Gaffney[b]

[a] *Graduate School of Environmental Sciences, Okayama University, Okayama 700-8530, Japan*
[b] *Centre for Mathematical Biology, Mathematical Institute, University of Oxford, Oxford OX1 3LB, UK*

Received: 30 September 2009 / Accepted: 1 March 2010 / Published online: 23 March 2010

Abstract Turing's pattern formation mechanism exhibits sensitivity to the details of the initial conditions suggesting that, in isolation, it cannot robustly generate pattern within noisy biological environments. Nonetheless, secondary aspects of developmental self-organisation, such as a growing domain, have been shown to ameliorate this aberrant model behaviour. Furthermore, while in-situ hybridisation reveals the presence of gene expression in developmental processes, the influence of such dynamics on Turing's model has received limited attention. Here, we novelly focus on the Gierer–Meinhardt reaction diffusion system considering delays due the time taken for gene expression, while incorporating a number of different domain growth profiles to further explore the influence and interplay of domain growth and gene expression on Turing's mechanism. We find extensive pathological model behaviour, exhibiting one or more of the following: temporal oscillations with no spatial structure, a failure of the Turing instability and an extreme sensitivity to the initial conditions, the growth profile and the duration of gene expression. This deviant behaviour is even more severe than observed in previous studies of Schnakenberg kinetics on exponentially growing domains in the presence of gene expression (Gaffney and Monk in Bull. Math. Biol. 68:99–130, 2006). Our results emphasise that gene expression dynamics induce unrealistic behaviour in Turing's model for multiple choices of kinetics and thus such aberrant modelling predictions are likely to be generic. They also highlight that domain growth can no longer ameliorate the excessive sensitivity of Turing's mechanism in the presence of gene expression time delays. The above, extensive, pathologies suggest that, in the presence of gene expression, Turing's mechanism would generally require a novel and extensive secondary mechanism to control reaction diffusion patterning.

Keywords Time delays · Growing domains · Gene expression · Turing pattern formation

*Corresponding author.
E-mail addresses: seirin.lee@gmail.com; seirin@ems.okayama-u.ac.jp (S. Seirin Lee).

1. Introduction

Cellular self-organisation drives biological morphogenesis in development and requires the exquisite and heterogeneous control of processes governing cell signalling, differentiation, proliferation and movement. Fundamental in this control is differential gene expression which is extensively regulated via cellular interactions that can be classified into two broad types. The first is cell-cell communication, a short range interaction via signalling between neighbouring cells as illustrated by Delta and Notch (Louvi and Artavanis-Tsakonas, 2006). The second is the use of long range signals, such as diffusible morphogen gradients, which provide a means of communicating over scales far exceeding that of the individual cell and exemplified by Dpp signalling in drosophila (Affolter and Basler, 2007; Chang et al., 2008).

The prospect of long range signalling by diffusible morphogens initiating large scale pattern formation has been contemplated since the initial work of Turing (1952). This demonstrated the physical plausibility of such a mechanism, providing two morphogens of differing diffusivities were present and that they interacted directly in a specific, well-characterised, manner commonly summarised as "short-range activation-long range inhibition" (Gierer and Meinhardt, 1972; Murray, 1993). Furthermore, the morphogen interactions that induce Turing's instability can be refined into two possible classes. The first is *pure* kinetics which in addition to short-range activation and long range inhibition, requires that the activator upregulates the inhibitor, which in turn downregulates the activator. In contrast, *cross* kinetics demands the converse activator-inhibitor interactions.

The Turing mechanism has been explored in numerous developmental settings, including vertebrate limb development (Miura and Shiota, 2000a, 2000b; Miura et al., 2006; Alber et al., 2008), embryonic feather branching (Harris et al., 2005) and zebrafish mesendoderm induction (Chen and Schier, 2002; Jing et al., 2006; Sakuma et al., 2002; Solnica-Krezel, 2003). However, despite such interest, establishing the molecular details of the interactions associated with a Turing mechanism has remained elusive. Nonetheless, numerous recent developmental studies emphasise the importance of gene expression. One illustration is the exploration of Nodal and Lefty zebrafish mesendodermal induction (Sakuma et al., 2002) which demonstrates that specific mRNA transcripts are dynamic, thus demonstrating the presence and regulation of gene expression in developmental processes.

It is not clear however that the indirect interaction of morphogens via the regulation of each other's gene expression can be represented by Turing's model. More generally, this concern illustrates that the Turing model approximates the details of morphogen-cell interactions at the level of morphogen interactions. The critical, largely unexplored, question is whether this is a legitimate approximation given the level of detail required in modelling large scale developmental patterning. However, gene expression is observed to be present and requires transcription and translation; this is noteworthy as these processes require the production of long polymeric molecules by the sequential addition of monomers, typically in the range of thousands to millions per gene. Hence delay processes are introduced into the feedback control the morphogens exert on each other in a Turing system. Estimates of the total extent of these delays range from 10 minutes to several hours, according to protein size and intron density (Lewis, 2003; Tennyson et al., 1995). Even though this may be shorter than timescales in many development events, though not necessarily in the rapid development of zebrafish for example, control systems are notoriously sensitive to delays which can have a disproportionate

influence. In such a potentially unstable system even small changes in the interaction dynamics may have a profound effect. As such, the Turing mechanism may not be robust to alterations in the details of the kinetics or the morphogen signalling pathways on the explicit introduction of gene expression.

It is not clear however that the indirect interaction of morphogens via the regulation of each other's gene expression can be represented by Turing's model. More generally, this concern illustrates that the Turing model approximates the details of morphogen-cell interactions at the level of morphogen interactions. The critical, largely unexplored, question is whether this is a legitimate approximation given the level of detail required in modelling large scale developmental patterning. However, the fact gene expression is observed to be present and requires transcription and translation, which in turn introduces a delay into the feedback control the morphogens exert on each other in a Turing system is noteworthy. Estimates of this delay range from 10 minutes to several hours, according to protein size and intron density (Lewis, 2003; Tennyson et al., 1995). Even though this may be shorter than timescales in many development events, though not necessarily in the rapid development of zebrafish for example, control systems are notoriously sensitive to delays which can have a disproportionate influence. In such a potentially unstable system even small changes in the interaction dynamics may have a profound effect. As such, the Turing mechanism may not be robust to alterations in the details of the kinetics or the morphogen signalling pathways on the explicit introduction of gene expression.

Initial investigations of such issues have been pursued by Gaffney and Monk (2006) and Seirin-Lee et al. (2010). In particular, the former explored the influence of gene expression time delays for activator production within the Schnakenberg (1979) model, an exemplar of cross kinetics. A number of features emerged: on fixed domains, Turing patterning did occur though with substantial increases in the patterning time. Thus, while spatial control was not adversely affected, one could observe an exquisite sensitivity of the patterning time with respect to the gene expression time delay; temporal control within such a system would be severely limited. On growing domains, once the gene expression delay was sufficiently large, initial condition sensitivity and Turing instability failure were also regularly observed. Nonetheless, there were regions of parameter space where spatially robust Turing-style patterns did emerge on growing domains, albeit with a sensitivity of the patterning time with respect to the gene expression time delay.

Seirin-Lee et al. (2010) considered gene expression time delays for both the activator and inhibitor dynamics of the pure kinetics, Gierer and Meinhardt (1972), model, on a stationary domain, plus the influence of different representations of the morphogen signalling pathways. While pattern initiation analogous to a standard Turing instability could be observed, albeit in restricted regions of parameter space and with a large patterning lag, self-organisation was also frequently accompanied by the development of oscillations and sensitivity to initial conditions. Furthermore, the details of the morphogen signalling pathway did greatly influence the dynamics.

Among many of the observations one can draw, note that the choice of interaction kinetics and the representation of the morphogen signalling do yield different results on a *stationary* domain. However, a detailed study of the choice of kinetics or the influence of morphogen signalling pathway dynamics on growing domains is still lacking. Nonetheless, domain growth is considered to be an important factor in numerous developmental scenarios, as exemplified by vertebrate limb development (Miura and Shiota, 2000a,

2000b; Miura et al., 2006; Hentschel et al., 2004). It is also important in processes associated with biological growth, such as alligator tooth morphogenesis (Kulesa et al., 1996) and the reorganisation of fish-markings (Kondo and Asai, 1995).

Domain growth is important theoretically due to another difficulty with the basic Turing model, namely that it exhibits sensitivity to fluctuations in the initial state of the system (Bard and Lauder, 1974; Bunow et al., 1980). This is certainly uncharacteristic of the exquisite control demanded of many developmental processes such as limb bud chondrogenesis. Domain growth has been shown to greatly ameliorate such sensitivity by inducing higher order patterns via a self-similar cascade of patterning rearrangement as the domain grows (Crampin et al., 1999). This cascade to robust self-organisation just requires an initial patterning which forms a central peak with domain growth; such features are commonly observed and virtually independent of the details of the Turing patterning kinetics in standard reaction diffusion models [ibid]. This mechanism of pattern formation has been observed in the Schnakenberg system in the presence of gene expression time delays leading to robust spatial patterning, though for restricted parameter choices (Gaffney and Monk, 2006). However, whether such cascades are inherited for other choices of interaction kinetics is unexplored once gene expression time delays are incorporated. Similarly, whether the details of the morphogen signalling pathway impact on such patterning dynamics is unknown. In particular, while the pattern initiation that can be observed in Seirin-Lee et al. (2010) for the Gierer–Meinhardt model on a stationary domain is necessary for such cascading pattern, it is by no means sufficient.

Thus in the following investigations we will consider an exemplar choice of *pure* morphogen interaction kinetics, namely Gierer and Meinhardt's (1972) model to specifically consider a fundamentally different choice of morphogen interactions compared to the Schnakenberg model. After introducing gene expression time delays, and two possible models of morphogen signalling transduction, we explore the resulting reaction diffusion dynamics on growing domains in one spatial dimension. Our focus will be to consider the extent reaction diffusion pattern formation on growing domains via self-similar cascades of pattern reorganisation is contingent on the morphogen interaction kinetics and the signal transduction dynamics once gene expression is considered.

2. Models on growing domains

The coupling between domain growth and development as well as numerous other biological self-organisation phenomena has motivated extensive studies of reaction diffusion patterning on growing domains (Arcuri and Murray, 1986; Bunow et al., 1980; Kondo and Asai, 1995; Varea et al., 1997; Madzvamuse, 2006; Madzvamuse et al., 2009). A systematic means of incorporating domain growth has been expounded for both uniform and heterogeneous growth (Crampin et al., 1999, 2002). The prospect that such dynamics may also be controlled by morphogen gradients has already been contemplated experimentally (Rogulja and Irvine, 2005) and theoretically (Neville et al., 2006), but this will be explored elsewhere in the context of incorporating sub-cellular dynamics and gene expression within reaction diffusion patterning models. Here we will develop models incorporating gene expression time delays and different morphogen signalling pathway dynamics on uniformly growing, one dimensional, domains for a system of Gierer–Meinhardt morphogens.

2.1. *Modelling gene expression time delays on growing domains*

Consider a uniformly growing one dimensional domain, $x \in [0, L_0 L(t)]$, where L_0 is the initial domain length and $L_0 L(t)$ is the domain length, an increasing function of time, with $L(0) = 1$. Let c_p denote the pth biochemical concentration, $p \in \{1, 2\}$, for a general two component reaction–diffusion system. On the above domain, standard conservation arguments give (Crampin et al., 1999)

$$\frac{\partial c_p}{\partial t} + \frac{\partial}{\partial x}\big(\alpha(x,t)c_p\big) = \sum_{q=1,2} \frac{\partial}{\partial x}\left(\mathcal{D}_{pq}\frac{\partial c_q}{\partial x}\right) + F_p\big(\boldsymbol{c}(x,t)\big),$$

where $F_p(\boldsymbol{c}(x,t))$ denotes the reaction kinetics, $\alpha(x,t)$ is the domain growth velocity field and $\mathcal{D}_{pq}$ are the components of a diffusion matrix. The latter is taken to be constant and diagonal below and is written in the form $\mathcal{D}_{pq} = \operatorname{diag}(\epsilon^2 D, D)$ with $\epsilon < 1$; this bound entails that c_1 has the shorter spatial range of the morphogens and is thus the activator.

Gene expression time delay models are influenced at location (x,t) by the gene expression instigated within the cells a time τ earlier, where τ is the gene expression time delay. However, due to domain growth, these cells were not at spatial location x at time $t-\tau$. Instead these cells were previously located at x_τ; an explicit expression can be found by backtracking along the characteristic generated by the velocity vector field starting at (x,t) (Gaffney and Monk, 2006). However, an explicit expression is not required below due to the consideration of Lagrangian coordinates.

In the presence of gene expression time delays, we thus have the reaction term $F_p(\boldsymbol{c}(x,t))$ generalises to

$$F_p\big(\boldsymbol{c}(x,t), \boldsymbol{c}(x_\tau, t-\tau)\big).$$

For convenience we relabel $(c_1, c_2) \to (u, v)$, and $(F_1, F_2) \to (f, g)$. We non-dimensionalise concentrations by $(\hat{u}, \hat{v}) = (Uu, Vv)$, length via $\hat{x} = x/L_0 \in [0, L(t)]$, time by $\hat{t} = t/T_S$, and the velocity vector field by $\hat{\alpha} = T_s\alpha/L_0$. Then the reaction diffusion system, with gene expression time delays, reduces to the form

$$\begin{aligned}
\frac{\partial u}{\partial t} + \alpha\frac{\partial u}{\partial x} &= \frac{\epsilon^2 T_s D}{L_0^2}\frac{\partial^2 u}{\partial x^2} + \gamma f\big(u(x,t), v(x,t), u(x_\tau, t-\tau), v(x_\tau, t-\tau)\big) - \frac{\partial \alpha}{\partial x}u,\\
\frac{\partial v}{\partial t} + \alpha\frac{\partial v}{\partial x} &= \frac{T_s D}{L_0^2}\frac{\partial^2 v}{\partial x^2} + \gamma g\big(u(x,t), v(x,t), u(x_\tau, t-\tau), v(x_\tau, t-\tau)\big) - \frac{\partial \alpha}{\partial x}v,
\end{aligned} \tag{1}$$

where γ is a constant and hats are dropped for convenience.

Following Crampin et al. (1999), consider Lagrangian coordinates (X,t) where X is the initial position of a tissue element moving with the flow α. The movement of tissue as a result of growth can be described in terms of the mapping between the Eulerian coordinate, x, and the Lagrangian coordinate X:

$$x = \Gamma(X,t), \qquad \Gamma(X,0) = X \in [0,1], \qquad \Gamma(0,t) = 0 \quad \text{for } t > 0.$$

Uniform growth implies $x = \Gamma(X,t) = XL(t)$ and hence

$$\alpha(x,t) = X\dot{L}(t) = x\frac{\dot{L}(t)}{L(t)} \tag{2}$$

with the fractional dilation rate given by

$$\frac{\partial \alpha}{\partial x} = \frac{\dot{L}(t)}{L(t)}.$$

Now we transform the spatial coordinates to the unit interval via the mapping

$$\big(x(t),t\big) \to \left(\frac{x(t)}{L(t)},t\right) = (\bar{x},t) \quad \text{where } \frac{x(t)}{L(t)} \in [0,1]. \tag{3}$$

Note that $x(t-\tau)/L(t-\tau) = X = x(t)/L(t)$ from (2). The fact the Lagrangian coordinate is time invariant, by construction, implies $\bar{x} = \bar{x}_\tau$. Thus on implementing the above mapping one finds

$$\big(u(x_\tau,t-\tau),v(x_\tau,t-\tau)\big) \xrightarrow{(3)} \big(u(\bar{x},t-\tau),v(\bar{x},t-\tau)\big) \stackrel{\text{def}}{=} (u_\tau,v_\tau).$$

In addition the first order convective terms cancel in the reaction diffusion equations. Hence the gene expression time delay system (1) can be expressed in the form

$$\begin{aligned}
\frac{\partial u}{\partial t} &= \frac{\epsilon^2 d}{L^2(t)}\frac{\partial^2 u}{\partial x^2} + \gamma f(u,v,u_\tau,v_\tau) - S(t)u,\\
\frac{\partial v}{\partial t} &= \frac{d}{L^2(t)}\frac{\partial^2 v}{\partial x^2} + \gamma g(u,v,u_\tau,v_\tau) - S(t)v,
\end{aligned} \tag{4}$$

where bars are once more dropped for convenience, $x \in [0,1]$, $d = T_s D/L_0^2$ and domain dilation also dictates the rate of biochemical dilution via $S(t) = \dot{L}(t)/L(t)$.

2.2. *Growth rate functions*

We consider three representative domain growth functions: exponential, logistic and linear, as summarised in Table 1.

Table 1 *The Growth Rate Functions*. The system of Eqs. (4) is considered for the growth rate functions below. $L_0 L(t)$ is the physical domain length, where L_0 is the initial domain length, and $S(t) = \dot{L}(t)/L(t)$ is the fractional dilation rate. The parameter $\delta > 0$ is a measure of the domain growth rate and $\xi > 0$ is the final size of the logistic growing domain

	$L(t)$	$S(t)$
Exponential growing domain	$\exp(\frac{\delta}{2}t)$	$\frac{\delta}{2}$
Logistic growing domain	$\frac{\exp(\delta t)}{1+(\exp(\delta t)-1)/\xi}$	$[\delta - \frac{\delta\exp(\delta t)}{\xi+\exp(\delta t)-1}]$
Linear growing domain	$1+\delta t$	$\frac{\delta}{1+\delta t}$

Table 2 *The Kinetics, Including Gene Expression Time Delays* (Seirin-Lee et al., 2010). Models I, II, I-S and II-S are given by combining Eqs. (4) with the kinetics listed below. Here, u and v are the activator and the inhibitor concentrations at (x,t), while u_τ and v_τ are the activator and the inhibitor concentrations at $(x,t-\tau)$, using the independent variables of Eqs. (4). The parameters a, b, c, κ are positive constants. Model I is based upon cell surface induction of signal transduction, whereas Model II requires ligand internalisation for signal transduction. Models I-S and II-S additionally incorporate the saturation of activator induced activator production. See text for further details

	$f(u,v,u_\tau,v_\tau)$	$g(u,v,u_\tau,v_\tau)$
Model I	$a-bu+\frac{u_\tau^2}{v_\tau}$	u_τ^2-v
Model II	$a-bu+3\frac{u_\tau^2}{v_\tau}-2\frac{u^2}{v}+c(u_\tau^2-u^2)$	u_τ^2-v
Model I-S	$a-bu+\frac{u_\tau^2}{(1+\kappa u_\tau^2)v_\tau}$	u_τ^2-v
Model II-S	$a-bu+3\frac{u_\tau^2}{(1+\kappa u_\tau^2)v_\tau}-2\frac{u^2}{(1+\kappa u^2)v}+c(u_\tau^2-u^2)$	u_τ^2-v

2.3. Gierer–Meinhardt kinetics

As summarised in Table 2, four models for the kinetics based on the Gierer and Meinhardt (1972) system are presented. A detailed motivation and derivation of these functions is given in Seirin-Lee et al. (2010); in the following section we present a summary, emphasising our interest in exploring the influence of sub-cellular dynamics on global pattern formation.

2.3.1. Sub-cellular dynamics

In particular, note that morphogens bind to cell surface receptors to induce signal transduction via protein- and lipid-mediated kinase cascades which subsequently modulate protein production via their influence on gene expression (Alberts et al., 2002). Endocytosis of receptor-ligand complexes is also commonly observed (Mukherjee et al., 1997) and is often considered to attenuate such signals (Beguinot et al., 1984; Wells et al., 1990; Sorkin and von Zastrow, 2002; Stoscheck and Carpenter, 2002). However, protein interactions in endosomes after ligand internalisation evidence the prospect that signal transduction may also be induced from the cell interior, via the endosomal membranes; examples include TGF-signalling in vertebrate cells and Dpp signalling in Drosophila (Entchev et al., 2000; Fischer et al., 2006; Piddini and Vincent, 2003; Roy and Wrana, 2005; Sorkin and von Zastrow, 2002).

Thus, we shall focus on one system, ultimately generating Model I below, where reversible ligand-receptor cell surface reactions instigate signal transduction. A second system, Model II below, instead requires irreversible binding and ligand internalisation for signal transduction. Analogous models, labelled I-S and II-S, additionally incorporate the saturation of activator induced activator production. All models also have an independent morphogen decay, representing a separate process of ligand internalisation without signalling. Considering the above, extreme, choices for the representation of morphogen signal transduction is sufficient to highlight whether sub-cellular dynamics will influence modelling outcomes.

2.3.2. The Gierer–Meinhardt model

To proceed, note that in the absence of gene expression time delays, the non-dimensionalised Gierer and Meinhardt (1972) model, with saturating kinetics, on a uniformly growing domain is given by

$$\begin{aligned}\frac{\partial u}{\partial t} &= \frac{\epsilon^2 d}{L^2(t)}\frac{\partial^2 u}{\partial x^2} + \gamma\left\{a - bu + \frac{u^2}{(1+\kappa u^2)v}\right\} - S(t)u,\\ \frac{\partial v}{\partial t} &= \frac{d}{L^2(t)}\frac{\partial^2 v}{\partial x^2} + \gamma\left\{u^2 - v\right\} - S(t)v.\end{aligned} \tag{5}$$

Here, a and b are positive constants which dictate the basal production rate and the decay rate of the activator whose concentration is u. The parameter $\kappa \geq 0$ controls the extent of saturation of activator-induced autocatalysis; when $\kappa = 0$, we have the standard Gierer–Meinhardt model.

In the following there is a slight abuse of notation with the same symbol representing the molecule and the non-dimensionalised concentration. One of non-linear, activator-inhibitor, interactions can be represented as activator autocatalysis

$$u + u \xrightarrow{\frac{\gamma}{[(1+\kappa u^2)v]}} 3u, \tag{6}$$

where the morphogen dependent rate parameter, $\gamma/[(1+\kappa u^2)v]$, represents inhibitor down-regulation of activator production, with activator saturation if $\kappa > 0$. The other reaction represents activator stimulated production of inhibitor, with a reaction constant γ:

$$u + u \xrightarrow{\gamma} 2u + v. \tag{7}$$

2.3.3. Models I, II, I-S & II-S

For Model I and Model I-S, we have the cell surface induction of signalling via reversible ligand-binding that ultimately, after a time delay τ, induces morphogen production. Here reactions (6) and (7) generalise to (Seirin-Lee et al., 2010)

$$u_\tau + u_\tau \xrightarrow{\frac{\gamma}{[(1+\kappa u_\tau^2)v_\tau]}} 2u_\tau + u, \tag{8}$$

$$u_\tau + u_\tau \xrightarrow{\gamma} 2u_\tau + v. \tag{9}$$

Here, in terms of the reaction participants, u_τ, u respectively denote a molecule of activator at time $t-\tau$ and time t, while v represents a molecule of inhibitor at time t. In contrast, within the reaction rate parameter $\gamma/[(1+\kappa u_\tau^2)v_\tau]$, we have a dependence on the concentrations of activator and inhibitor at time $t-\tau$, via u_τ, v_τ. Thus, the production of activator at time t is due to non-linear interactions at time $t-\tau$ via molecules that interact reversibly, which is assumed to take place via receptor binding at the cell surface. Standard balance arguments for these interactions, additionally incorporating the zeroth and first order linear interactions of the Gierer–Meinhardt system summarised by Eqs. (5), then yield the kinetics functions, f, g, for Model I-S, as presented in Table 2. Further, setting $\kappa = 0$ yields Model I.

In contrast, for Models II and II-S, irreversible binding at the cell surface, followed by internalisation, is required for the induction of signal, the resulting gene expression and ultimately morphogen production. With the same notation used above in reactions (8), (9) we have that reactions (6) and (7) generalise to [ibid]

$$u_\tau + u_\tau \xrightarrow{\frac{\gamma}{[(1+\kappa u_\tau^2)v_\tau]}} 3u,$$

$$u_\tau + u_\tau \xrightarrow{\gamma} 2u + v.$$

Thus, for example, the activator morphogen molecules inducing the autocatalytic signal are internalised for the duration of gene expression. As mentioned, exploring the above two different, extreme, representations of the signal transduction dynamics will indicate whether such dynamics influences model predictions. Standard balance arguments, in combination with the zeroth and first order kinetics of the Gierer–Meinhardt system yield Model II-S, as given in Table 2 while setting $\kappa = 0$, reveals Model II. Finally, note that all the above models reduce to the Gierer–Meinhardt system summarised by Eq. (5) as the gene expression time delay, τ, tends to zero.

2.4. Initial and boundary conditions

2.4.1. Zero flux boundary conditions

Arcuri and Murray (1986) and Dillon et al. (1994) have investigated the influence of boundary conditions on the sensitivity of pattern selection and stability. They demonstrated that zero flux boundary conditions impose the weakest constraint on pattern formation and lead to the greatest difficulty in achieving reliable patterning. As such, zero flux conditions are the most appropriate for considering the role of domain growth in stabilising pattern selection. In addition, zero flux boundary conditions have the natural interpretation of no morphogen loss at the domain boundary and thus we impose

$$\frac{\partial u}{\partial x} = \frac{\partial v}{\partial x} = 0 \quad \text{at } x = 0, 1.$$

2.4.2. Initial conditions

We consider initial conditions which are small perturbations of the homogeneous steady state (u_*, v_*) in the absence of domain growth. We typically use two types of initial conditions: a time independent initial condition, labelled IC1, and a time dependent initial condition, labelled IC2. In detail, for $t \in [0, \tau]$,

$$\text{IC1:} \quad u(x,t) = u_* + \phi_u(x), \qquad v(x,t) = v_* + \phi_v(x), \tag{10}$$

$$\begin{aligned} \text{IC2:} \quad u(x,t) &= \big(u_* + \phi_u(x)\big)\big[1 + 0.0025\cos\big(\pi t/(2\tau)\big)\cos(\pi x)\big], \\ v(x,t) &= \big(v_* + \phi_v(x)\big)\big[1 + 0.0025\cos\big(\pi t/(2\tau)\big)\cos(\pi x)\big] \end{aligned} \tag{11}$$

where

$$\begin{aligned} \phi_u(x) = 0.00125x^5\big(1 - x^2\big)\big(&-170.6666682x^3 + 412.4444479x^2 - 312.8888910x \\ &+ 71.1111113\big), \end{aligned}$$

$$\phi_v(x) = 0.00600x^5\left(1-x^2\right)\left(-130.8444445x^3 + 337.0666669x^2 - 281.6000002x + 75.3777778\right).$$

The precision of the coefficients is to ensure consistency of the boundary and initial conditions so as to avoid unnecessary mathematical and numerical complications; it is not indicative of a general model fine tuning.

2.5. *Reference parameter set*

In Table 3 we present reference parameter values that are typically used for the simulations below. Parameter set I is used for Models I-S and II-S, while parameter set II is used for Models I and II. The initial physical domain size is taken to 10^{-2} cm which is approximately 10 cell lengths; thus the scaled domain size of unity in the figures corresponds to a physical size of 10^{-2} cm. In addition, note the invariance of the non-dimensionalised equations with respect to the transformation $L_0 \to \psi L_0$, $T_s \to \psi^2 T_s$. Consequently, the solutions below in fact correspond to one parameter families of solutions, generated by changing ψ.

Table 3 *Parameter Sets for Models I, II, I-S and II-S*. The physical domain size is taken to be 10^{-2} cm which is approximately 10 cell lengths. A range of gene expression time delays are considered, up to 50 minutes in duration. Use of set I below corresponds to the use of the common parameters, plus those specifically listed under set I; analogously for parameter set II. Note these parameters also correspond to a family of dimensional solutions, as detailed in Section 2.5

Parameter	Value
Physical initial domain size (L_0, cm)	10^{-2}
Diffusivity of the inhibitor (D, cm^2/sec)	10^{-6}
Ratio of diffusion coefficients (ϵ^2)	$\{10^{-2}, 10^{-3}\}$
Dimensional time scale (T_s, seconds)	100
Nondimensional diffusivity of the inhibitor (d)	1
Exponential domain growth rate (δ_{exp})	{0.0008, 0.0015, 0.0016}
Linear domain growth rate (δ_{lin})	{0.00055, 0.0011}
Logistic domain growth rate ($\delta_{\log}$)	0.00085
Final size of Logistic domain (ξ, 10^{-2} cm)	25
Set I	
Base production rate of the activator (a)	0.128
Decay rate of the activator (b)	0.667
Activator reaction rate to produce inhibitor (c)	42.667
Nondimensional reaction rate parameter (γ)	0.75
Activator induced saturation (κ)	0.1
Gene expression time delay (τ, 10^2 sec)	{0.0, 0.12, 0.15, 0.6, 1.1, 1.2, 7.2, 24}
Homogeneous steady state (u_*, v_*)	(1.43566, 2.06112)
Set II	
Base production rate of the activator (a)	0.1
Decay rate of the activator (b)	0.5
Activator reaction rate to produce inhibitor (c)	1.0
Nondimensional reaction rate parameter (γ)	0.2
Activator induced saturation (κ)	0.0
Gene expression time delay (τ, 10^2 sec)	{0.0, 7.2, 15, 30}
Homogeneous steady state (u_*, v_*)	(2.2, 4.84)

2.5.1. The timescale of domain growth

Domain growth is considered to be driven by cell proliferation and thus occurs on the timescale of the cell cycle; a reasonable timescale for domain doubling assuming fast cell division is 24 hours (Abdreeff et al., 2000). Note that biochemical reaction timescales are typically considered to be much faster, on the scale of seconds or minutes whereas the diffusive timescale can be approximated by $L_0^2/D \sim 100$ seconds for the parameter values in Table 3; hence we are in the slow growth regime.

Noting the representative domain doubling time of 1 day, and that a convenient timescale is $T_s \sim L_0^2/D = 100$ seconds, we have the following estimates of the non-dimensionalised growth rate parameter δ for each of the growth regimes listed in Table 2:

Exponential domain growth rate: $\delta_{\text{exp}} \approx 0.0016$,

Linear domain growth rate: $\delta_{\text{lin}} \approx 0.0011$,

Logistic domain growth rate: $\delta_{\text{log}} \approx 0.00085$.

Note that logistic growth rate parameter is determined by enforcing a domain doubling in the first 24 hours, given growth saturation occurs at 25 times the initial domain size, so that $\xi = 25$ in Table 1. Additional values of the domain growth rate are also briefly considered below.

2.6. Numerical methods

The model equations are a coupled set of parabolic partial differential equations on a fixed one-dimensional spatial domain, with non-autonomous terms and a time delay. They are solved via an implicit numerical scheme, storing the history of the model constituents as required to track the time-delayed variables.

3. Results

A direct generalisation of the calculations presented by Gaffney and Monk (2006) once more reveals that the equations of a linearised stability analysis for the models summarised by Eq. (4) and Table 2 do not admit temporal oscillations at the Turing bifurcation point.

The results presented below are numerical, using the parameters from Table 3 throughout this section. Figure 1 depicts the results of the saturation Model II-S, and thus represents the dynamics associated with ligand internalisation morphogen-cell interactions. In contrast, in Fig. 2 results are presented for the saturation Model I-S, which considers cell surface, reversible ligand binding, morphogen-cell interactions. Finally, Fig. 3 plots the results for Models I and II, where there is no longer the saturation of activator induced activator production. Results with no gene expression time delay are presented in Figs. 1(a), 1(b), 1(c), Fig. 2(a) and Figs. 3(a), 3(b), 3(c). In the absence of gene expression dynamics, we have always found a self-similar patterning cascade that is effectively independent of the details of the initial condition perturbations, consistent with the results detailed by Crampin et al. (1999).

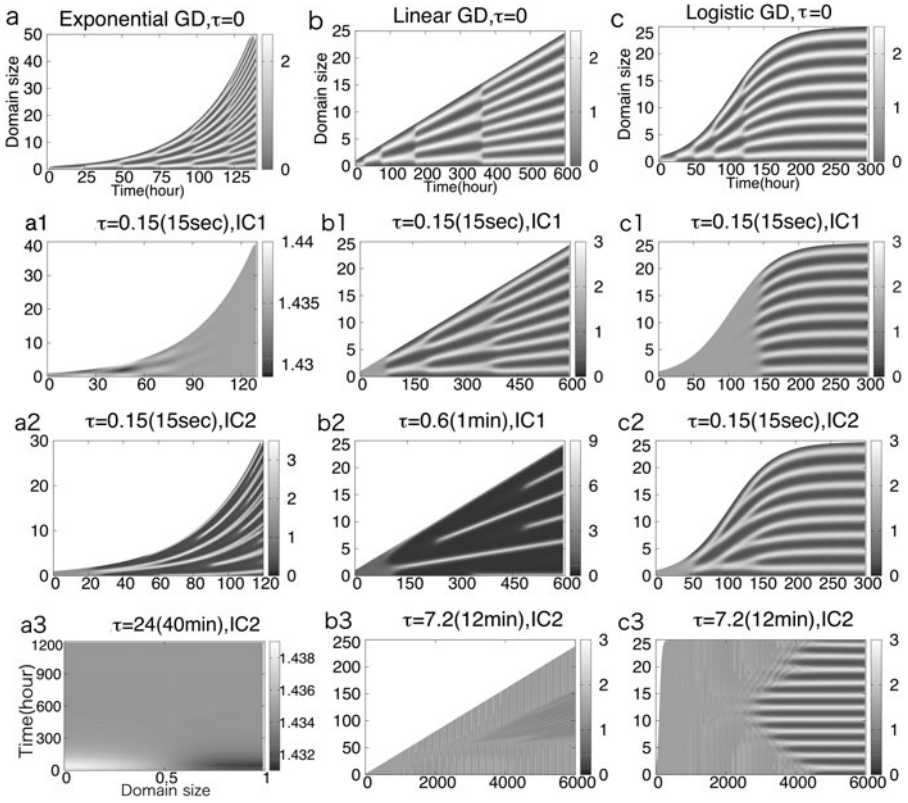

Fig. 1 Model II-S. In the above plots results are presented for Model II-S, which possesses ligand internalisation dynamics and saturating activator induced activator production. Parameter set I in Table 3 is used for these plots with the ratio of diffusion coefficients given by $\epsilon^2 = 10^{-2}$. With exception of (a3), the horizontal axis in all plots represents time in units of hours, and the vertical axis gives the domain size, in units of the initial domain length which corresponds to 10^{-2} cm or approximately 10 cell lengths. These axes are also common to Figs. 2 and 3. Exponential, linear and logistic growth profiles are considered with the respective growth rates $\delta_{\text{exp}} = 0.0016$, $\delta_{\text{lin}} = 0.0011$ and $\delta_{\text{log}} = 0.00085$, which correspond to a doubling time of approximately 24 hours (see Section 2.5.1). IC1 denotes the initial condition (10) and IC2 refers to the initial condition (11). Also, the non-dimensionalised gene expression time delay, τ, is given above each plot with its dimensional size in brackets. The axes of (a3) are different for clarity. This plot is for exponential growth with a doubling time of approximately 24 hours; the non-dimensionalised Lagrangian spatial coordinate is used for the horizontal axis and the vertical axis is in units of hours, once more using the timescale $T_s = 100$ seconds in Table 3.

3.1. The ligand internalisation models: Model II and Model II-S

Sensitivity to initial conditions, irregular patterning and patterning failure In the absence of subcellular and gene expression dynamics, the most notable feature of reaction diffusion pattern formation on growing domains has been the robust selection of higher modes via a cascade of pattern reorganisation, regardless of fluctuations in the initial conditions. However, our results for the ligand internalisation Models, II and II-S, demon-

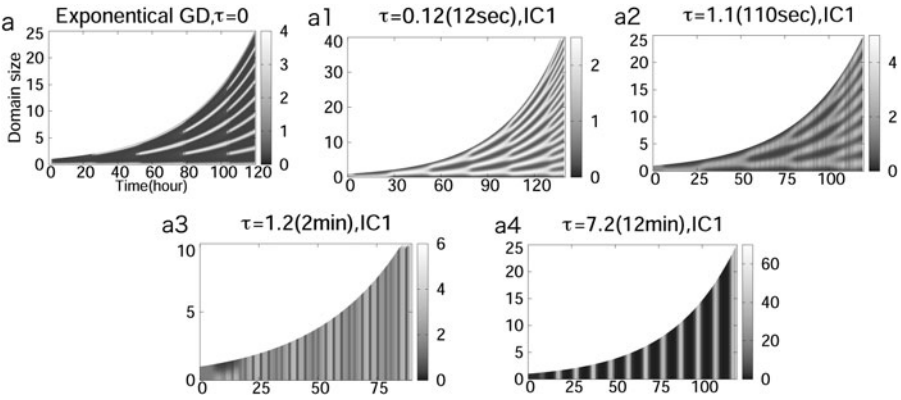

Fig. 2 Model I-S. In the above plots results are presented for Model I-S, where morphogen-cell interactions are instigated on the cell surface via reversible ligand binding, with saturation of activator induced activator production. Parameter set I in Table 3 is used with a ratio of diffusion coefficients given by $\epsilon^2 = 10^{-3}$. The horizontal axis in all plots represents time, in units of hours, and the vertical axis gives the domain size, in units of the initial domain length which corresponds to 10^{-2} cm or approximately 10 cell lengths. The label IC1 denotes the initial condition (10). The domain is exponentially growing with a growth parameter of $\delta_{\text{exp}} = 0.0015$ which corresponds to a doubling time of approximately 25 hours using the timescale $T_s = 100$ seconds in Table 3. Finally note that the non-dimensionalised gene expression time delay, τ, is given above each plot with its dimensional size in brackets.

strate the general loss of this mechanism for the robust generation of pattern on consideration of gene expression time delays. For example, perturbations of the initial conditions can invoke a failure of the Turing instability in one case and patterning in another, as illustrated by Figs. 1(a1) and 1(a2), even for an unrealistically small gene expression time delay (of about 15 seconds for the parameters used). The fact the very prospect of patterning is sensitive to perturbations in the initial conditions is a level of sensitivity that has not been observed in previous studies (Gaffney and Monk, 2006). Further, even when the final pattern appears to be similar for different initial conditions, the temporal profile of the patterning can be very sensitive to the initial conditions, as illustrated by Figs. 1(c1) and 1(c2).

It is important to note that when patterning does occur, it is typically not via the self-similar cascade characterising the self-organisation in the absence of gene expression time delays. This is illustrated by comparing Figs. 1(a), 1(a2) or Figs. 1(b), 1(b2). More generally, while Fig. 3(b1) and other plots may appear to be exhibit reasonable pattern formation dynamics, the mechanism by which pattern is generated nonetheless lacks robustness as explicitly illustrated for other plots in this section.

Further, consider Model II, which has ligand internalisation but no activator saturation, in the case when gene expression dynamics are absent. In Figs. 3(b) and 3(c), one can observe the number of peaks increasing in powers of two (noting the half-peaks at the domain edge count as only one peak). However, on considering gene expression time delays the self-similar peak rearrangements are lost once more, as illustrated by Figs. 3(b1), 3(b2) and Figs. 3(c1), 3(c2). Finally, the Turing instability generally fails for the ligand internalisation models on increasing the gene expression time delay, as illustrated in

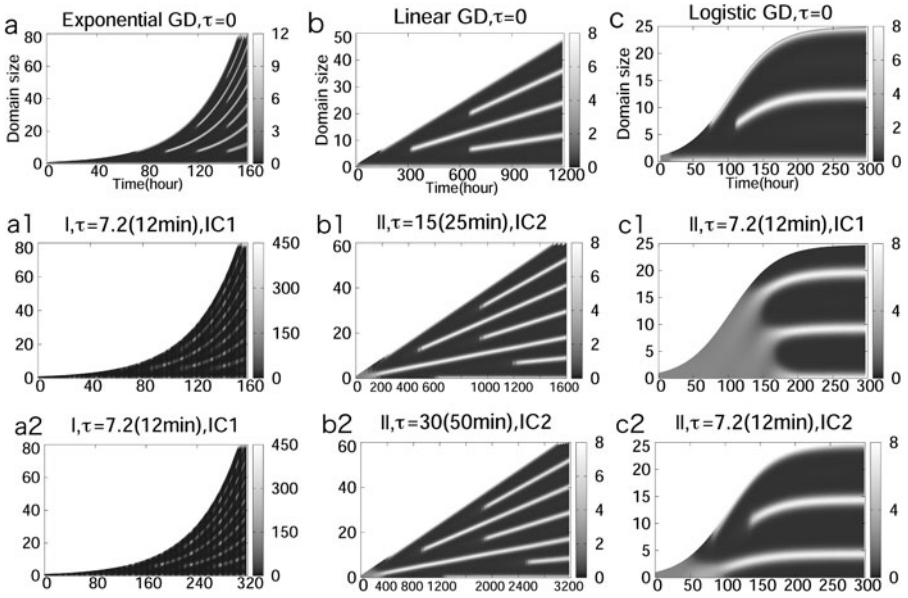

Fig. 3 Models I and II. In the above plots results are presented for Models I, II which lack saturating activator induced activator production ($\kappa = 0$). The horizontal and vertical axes are the same as those used in Figs. 1 and 2 (with the exception of Fig. 1(a3)); the horizontal axis represents time in units of hours and the vertical axis is the domain size in units of the initial domain length. The non-dimensionalised gene expression time delay, τ, is given above each plot with its dimensional size in brackets together with the label I for Model I results and analogously for Model II. The labels IC1 and IC2 respectively refer to the initial conditions (10) and (11). In plots (a–a2) we have Model I which corresponds to cell surface reversible ligand binding of morphogen. For these plots, parameter set II in Table 3 is used with a ratio of diffusion coefficients given by $\epsilon^2 = 10^{-3}$. The domain is exponentially growing with a growth parameter $\delta_{\text{exp}} = 0.0016$ in plots (a) and (a1) and $\delta_{\text{exp}} = 0.0008$ in plot (a2) which respectively correspond to doubling times of approximately 24 hours and 48 hours, using the timescale $T_s = 100$ seconds in Table 3. In the remaining graphs, results are presented from Model II, which corresponds to morphogen-cell interactions being driven by ligand internalisation. Parameter set II in Table 3 is used once more, though the ratio of the diffusion coefficients is $\epsilon^2 = 10^{-2}$. Further, in plots (b–b2) we have linear growth with $\delta_{\text{lin}} = 0.0011$ in plots (b), (b1) and $\delta_{\text{lin}} = 0.00055$ in plot (b2). In contrast, for plots (c), (c1) and (c2) we have logistic growth; the growth parameters are $(\delta_{\log}, \xi) = (0.00085, 25)$ for all these plots. The domain doubling time is approximately 24 hours for all plots except for (a2) and (b2), where it is approximately 48 hours, as detailed in Section 2.5.1.

Fig. 1(a3) and as previously observed for Schnakenberg kinetic models on exponentially growing domains (Gaffney and Monk, 2006).

The patterning lag and sensitivity to the gene expression time delay The presence of gene expression time delays sensitises the timing of the onset of patterning to fluctuations in the initial conditions for ligand internalisation models. This novel observation is illustrated by Figs. 1(c1), (c2) and also by Figs. 3(c1), (c2). As expected from previous studies (Seirin-Lee et al., 2010), small increases in the gene expression time delay radically increase the time to patterning as highlighted in all plots in Fig. 1 where patterning occurs with a non-zero gene expression time delay. Examining Fig. 1(c3) for example illustrates that a 12 minute gene expression time delay induces a patterning lag of approximately

2500 hours. This also reinforces the sensitivity of the patterning lag with respect to the gene expression time delay observed previously [ibid] and clearly further demonstrated by examining the effects of increasing the time delay in Fig. 1.

Sensitivity to the growth profile Note that in the absence of time delays, one can observe that the self-similar patterning cascade occurs regardless of the growth profile. This yields a pattern which is semi-scale invariant though, ultimately, it is dictated by the domain size, as observed in Figs. 1(a), 1(b), 1(c). This is generally observed provided one does not fix the final domain size of saturating growth to be extremely close to the domain size where pattern rearrangement is induced, which requires exquisite parameter fine tuning (Crampin et al., 1999). In contrast, comparing Figs. 1(a1), 1(b1), 1(c1) 1(a2), 1(c2) reveals that even unrealistically small gene expression time delays can profoundly sensitise patterning to the growth profile, even to the point where patterning can occur with some growth profiles, but not with others.

3.2. The reversible ligand binding models: Model I and Model I-S

Recall that Model I corresponds to morphogen-cell interactions via reversible ligand binding on the cell surface without activator saturation; this behaves rather differently. There is clearly an instability driving the system away from the homogeneous steady state and, in the absence of gene expression time delays, this drives the self-similar cascade of peak insertions depicted in Fig. 3(a). However, as observed on stationary domains (Seirin-Lee et al., 2010), increasing the gene expression time delay, even within biologically reasonable bounds, results in the emergence of oscillations with extremely large peaks in the activator, as shown in Figs. 3(a1), 3(a2).

Consequently, we focus on Model I-S which additionally has saturation of activator induced activator production. In the absence of time delays this model once more reproduces a self-similar cascade of peak insertion patterning. For very small gene expression time delays one instead finds a self-similar cascade of peak splitting; this is depicted in Figs. 2(a), 2(a1). As the gene expression time delay is increased even slightly, temporal oscillations occur and the self-similar cascade, and indeed all spatial structure, is lost as illustrated in Figs. 2(a3), 2(a4). This also occurs for linear and logistic growth (results not shown). In contrast to the ligand internalisation models, the patterning lags and sensitivity are not as profound, but the loss of spatial structure entails that patterning cannot emerge regardless.

Finally, note that despite the fact both representations of the gene expression and subcellular dynamics predict the instability of the homogeneous steady state, the nature of the behaviour is very different. It is also very different from the dynamics of the Schnakenberg model in the presence of time delays (Gaffney and Monk, 2006).

4. Discussion and conclusions

We have constructed a model for morphogen interactions based upon the Gierer and Meinhardt (1972) model on one dimensional, uniformly growing domain. We have additionally considered representations for the sub-cellular dynamics and gene expression in the form

of models based on ligand internalisation, Model II and Model II-S, or reversible ligand binding at the cell surface, Model I and Model I-S. While we have noted that linear theory does not predict the presence of oscillations, they can in fact occur with a suitable choice of the sub-cellular dynamics. This reinforces previous observations by Gaffney and Monk (2006) and Seirin-Lee et al. (2010) that linear theory is unreliable in the presence of gene expression time delays and that sub-cellular and gene expression dynamics cannot be neglected in models of morphogen driven pattern formation.

Crampin et al. (1999) has been among previous studies advocating that domain growth can ameliorate the sensitivity of reaction diffusion self-organisation to noise in the initial conditions by initiating a self-similar cascade of patterning. However, even for very small gene expression time delays this cascade is lost for Gierer–Meinhardt kinetics. In particular, for models based on reversible ligand binding, the initial evolution away from the homogeneous steady state results in temporal oscillations without spatial structure for reasonable estimates of the gene expression time delay. In contrast, models based on ligand internalisation exhibit extreme sensitivity to the growth profile, the size of the gene expression time delay and the initial conditions, even to the extent of determining the presence or absence of self-organisation. Thus, we have that the homogeneous steady state is typically unstable in the presence of gene expression delays which yields the possibility of self-organisation. However, the concerns over the lack of model robustness espoused by numerous authors, such as Bard and Lauder (1974) and Bunow et al. (1980), re-emerge with vigour for reaction diffusion patterning, even on growing domains, once gene expression time delays are considered.

Further difficulties are apparent. In particular, the spatially homogeneous temporal oscillations observed in the reversible ligand binding models cannot drive spatial pattern formation and possess unreasonable oscillation amplitudes in the absence of explicit activator saturation. In addition, patterning consistently fails for the ligand internalisation models once the gene expression time delay is sufficiently large, while for smaller gene expression time delays the patterning lag is unreasonably large. These pathological behaviours of the Gierer–Meinhardt model are even more severe than for the Schnakenberg model explored for exponential growth in Gaffney and Monk (2006). While pattern formation by self-similar cascades can occur on growing domains for restricted regions of parameter space for the latter, such behaviour has not been found for the Gierer–Meinhardt model given parameter values typifying biochemical diffusion rates, developmental growth and gene expression time delays.

Our results emphasise that previously observed pathologies are not limited to a special choice of kinetics or representation of the gene expression dynamics and are therefore more likely to be generic. Nonetheless, different choice of kinetics and sub-cellular dynamics do yield different modelling predictions. Hence we also no longer have the expectation that all systems exhibiting a Turing instability will behave in a remotely similar way on a growing domain given gene expression dynamics. This is also important in constructing models of developmental self-organisation on growing domains, as it is clear that choosing the simplest kinetics, a common strategy as illustrated in Miura et al. (2006), is inappropriate. Further, investigations of the Turing space for a given choice of kinetics, even for growing domains, such as those derived and considered in Alber et al. (2008) for limb self-organisation, should assess numerous additional factors given the presence of gene expression. These include the prospect of excessive patterning lags, the possibility of oscillations and extreme sensitivity, to the initial conditions, to the domain

growth profile, to the representation of the signal transduction dynamics and, finally, to the duration of the gene expression time delay.

The accumulation of results illustrating pathological behaviours for reaction diffusion patterning in the presence of gene expression time delays does increasingly suggest a very limited prospect of finding Turing's mechanism in developmental systems requiring exquisite control in the presence of gene expression. At best, one must consider a restricted choice of kinetics and parameters, while the Gierer–Meinhardt model is clearly inappropriate on growing domains. It is also clear that studies implementing a Turing system in development do need to address the influence of sub-cellular dynamics and whether one can control or remove the deviant behaviour that has been observed in the present study and previous ones (Gaffney and Monk, 2006; Seirin-Lee et al., 2010). This is especially true given such behaviour has persisted or intensified on the addition of domain growth, which has previously been considered to reduce the difficulties associated with Turing's mechanism. Numerous applications of reaction diffusion modelling are subject to such reevaluation. This includes zebrafish mesendoderm induction, where in-situ hybridisation explicitly indicates the importance of gene expression (Sakuma et al., 2002; Solnica-Krezel, 2003), and models of limb development, where reaction diffusion patterning on growing domains have been extensively considered (for example Miura and Shiota, 2000a; Hentschel et al., 2004; Newman and Muller, 2005; Miura et al., 2006; Alber et al., 2008).

This raises an interesting and important paradox: Turing's model does reproduce qualitative biological observations that can otherwise be difficult to explain in development yet the mechanism is inordinately sensitive to gene expression dynamics. This motivates explorations for either a novel, stabilising, secondary mechanism that supplements the simple Turing model such as, possibly, cellular chemotaxis, or analogous, but ultimately different, mechanisms for developmental pattern formation. One example of the latter is based on adhesion dynamics, as suggested by Zeng et al. (2004) in the context of limb development.

The application of Turing's model in fish skin marking self-organisation has been suggested (Kondo and Asai, 1995), though recent experiments stress a different interpretation of Turing patterning, whereby cells form the main constituents of the model rather than morphogens (Kondo et al., 2009; Nakamasu et al., 2009). Nonetheless, responses in the rate of cell production or apoptosis to extracellular signals are likely to suffer from delays in such models. Thus, while we have not explored fish markings in detail for the present study, it does raise the possibility that Turing's mechanism, or simple generalisations thereof, may also suffer from the difficulties we have observed despite the novel model interpretation. Thus we conclude by suggesting that the models of the cell-cell interactions that are under development to explore fish markings, such as those by Uriu and Iwasa (2007) or Nakamasu et al. (2009), should also be assessed for sensitivity to delays arising due to gene expression and cell dynamics.

Acknowledgements

This publication is based on work supported in part by Award No. KUK-C1-013-04, made by King Abdullah University of Science and Technology (KAUST). SSL gratefully acknowledges funding from The Japan Society for The Promotion of Science (JSPS Fellowship DC1).

References

Abdreeff, M., Goodrich, D.W., Pardee, A.B., 2000. Cell proliferation, differentiation and apoptosis. In: The Holland-Frei Cancer Medicine, 5th edn. BC Decker, Hamilton, Chap. 2.

Affolter, M., Basler, K., 2007. The Decapentaplegic morphogen gradient: from pattern formation to growth regulation. Nat. Rev. Genet. 8, 663–674.

Alber, M., Glimm, T., Hentschel, H., Kazmierczakd, B., Zhanga, Y., Zhua, J., Newman, S., 2008. The morphostatic limit for a model of skeletal pattern formation in the vertebrate limb. Bull. Math. Biol. 70, 460–483.

Alberts, B., Johnson, A., Walter, P., Lewis, J., Raff, M., Roberts, K., 2002. Molecular Biology of the Cell. 5th edn. Garland, New York.

Arcuri, P., Murray, J.D., 1986. Pattern sensitivity to boundary and initial conditions in reaction-diffusion models. J. Math. Biol. 24, 141–165.

Bard, J., Lauder, I., 1974. How well does Turing's theory of morphogenesis work? J. Theor. Biol. 45, 501–531.

Beguinot, L., Lyall, R.M., Willingham, M.C., Pastan, I., 1984. Down-regulation of the epidermal growth factor receptor in KB cells is due to receptor internalization and subsequent degradation in lysosomes. Proc. Natl. Acad. Sci. 81, 2384–2388.

Bunow, B., Kernevez, J.P., Joly, G., Thomas, D., 1980. Pattern formation by reaction–diffusion instabilities: applications to morphogenesis in *drosophila*. J. Theor. Biol. 84, 629–649.

Chang, W., Liou, W., Pen, H., Chou, H., Chang, Y., Li, W., Chiang, W., Pai, L., 2008. The gradient of Gurken, a long-range morphogen, is directly regulated by Cbl-mediated endocytosis. Development 135, 1923–1933.

Chen, Y., Schier, A., 2002. Lefty proteins are long-range inhibitors of squint-mediated nodal signaling. Curr. Biol. 12, 2124–2128.

Crampin, E.J., Gaffney, E.A., Maini, P.K., 1999. Reaction and diffusion on growing domains: scenarios for robust pattern formation. Bull. Math. Biol. 61, 1093–1120.

Crampin, E.J., Hackborn, W.W., Maini, P.K., 2002. Pattern formation in reaction–diffusion models with nonuniform domain growth. Bull. Math. Biol. 64, 747–769.

Dillon, R., Maini, P.K., Othmer, H.G., 1994. Pattern formation in generalized Turing systems I. Steady-state patterns in systems with mixed boundary conditions. J. Math. Biol. 32, 345–393.

Entchev, E.V., Schwabedissen, A., Gonzalez-Gaitan, M., 2000. Gradient formation of the TGF-β homolog Dpp. Cell 103, 981–991.

Fischer, J.A., Eun, S.H., Doolan, B.T., 2006. Endocytosis, endosome trafficking, and the regulation of drosophila development. Annu. Rev. Cell Dev. Biol. 22, 181–206.

Gaffney, E.A., Monk, N.A.M., 2006. Gene expression time delays and Turing pattern formation systems. Bull. Math. Biol. 68, 99–130.

Gierer, A., Meinhardt, H., 1972. A theory of biological pattern formation. Kybernetik 12, 30–39.

Harris, M.P., Williamson, S., Fallon, J.F., Meinhardt, H., Prum, R.O., 2005. Molecular evidence for an activator–inhibitor mechanism in development of embryonic feather branching. Proc. Natl. Acad. Sci. USA 102(33), 11734–11739.

Hentschel, H.G.E., Glimm, T., Glazier, J.A., Newman, S.A., 2004. Dynamical mechanisms for skeletal pattern formation in the vertebrate limb. Proc. R. Soc. Lond. B 271, 1713–1722.

Jing, X.H., Zhou, S.M., Wang, W.Q., Chen, Y., 2006. Mechanisms underlying long- and short-range nodal signaling in zebrafish. Mech. Dev. 123, 388–394.

Kondo, S., Asai, R., 1995. A reaction-diffusion wave on the skin of the marine angelfish *Pomacanthus*. Nature 376, 765–768.

Kondo, S., Iwashita, M., Yamaguchi, M., 2009. How animals get their skin patterns: fish pigment pattern as a live Turing wave. Int. J. Dev. Biol. 53, 851–856.

Kulesa, P.M., Cruywagen, G.C., Lubkin, S.R., Maini, P.K., Sneyd, J., Ferguson, M.W.J., Murray, J.D., 1996. On a model mechanism for the spatial patterning of teeth primordia in the *Alligator*. J. Theor. Biol. 180, 287–296.

Lewis, J., 2003. Autoinhibition with transcriptional delay: a simple mechanism for the zebrafish somitogenesis oscillator. Curr. Biol. 13, 1398–1408.

Louvi, A., Artavanis-Tsakonas, S., 2006. Notch signalling in vertebrate neural development. Nat. Rev. 7, 93–102.

Madzvamuse, A., 2006. Time-stepping schemes for moving grid finite elements applied to reaction-diffusion systems on fixed and growing domains. J. Comput. Phys. 214, 239–263.

Madzvamuse, A., Gaffney, E.A., Maini, P.K., 2009. Stability analysis of non-autonomous reaction-diffusion systems: the effects of growing domains. J. Math. Biol. doi:10.1007/s00285-009-0293-4.
Miura, T., Shiota, K., 2000a. Extracellular matrix environment influences chondrogenic pattern formation in limb bud micromass culture: experimental verification of theoretical models. Anat. Rec. 258, 100–107.
Miura, T., Shiota, K., 2000b. TGFβ2 acts as an activator molecule in reaction–diffusion model and is involved in cell sorting phenomenon in mouse limb micromass culture. Dev. Dyn. 217, 241–249.
Miura, T., Shiota, K., Morriss-Kay, G., Maini, P.K., 2006. Mixed-mode pattern in Doublefoot mutant mouse limb-Turing reaction–diffusion model on a growing domain during limb development. J. Theor. Biol. 240, 562–573.
Mukherjee, S., Ghosh, R.N., Maxfield, F.R., 1997. Endocytosis. Physiol. Rev. 77(3), 759–803.
Murray, J.D., 1993. Mathematical Biology, 2nd edn. Springer, Berlin.
Nakamasu, A., Takahashi, G., Kanbe, A., Kondo, S., 2009. Interactions between zebrafish pigment cells responsible for the generation of Turing patterns. Proc. Natl. Acad. Sci. USA 106, 8429–8434.
Neville, A., Matthews, P., Byrne, H., 2006. Interactions between pattern formation and domain growth. Bull. Math. Biol. 68(8), 1975–2003.
Newman, S., Muller, G., 2005. Origination and innovation in the vertebrate limb skeleton: an epigenetic perspective. J. Exp. Zool. B (Mol. Dev. Evol.) 304, 593–609.
Piddini, E., Vincent, J., 2003. Modulation of developmental signals by endocytosis: different means and many ends. Curr. Cell Biol. 15, 474–481.
Rogulja, D., Irvine, K.D., 2005. Regulation of cell proliferation by a morphogen gradient. Cell 123, 449–461.
Roy, C.L., Wrana, J.L., 2005. Clathrin- and nonclathrin-mediated endocytic regulation of cell signaling. Nat. Rev. Mol. Cell Biol. 6, 112–126.
Sakuma, R., Ohnishi, Y., Meno, C., Fujii, H., Juan, H., Takeuchi, J., Ogura, T., Li, E., Miyazono, K., Hamada, H., 2002. Inhibition of nodal signalling by lefty mediated through interaction with common receptors and efficient diffusion. Genes Cells 7, 401–412.
Schnakenberg, J., 1979. Simple chemical reaction systems with limit cycle behaviour. J. Theor. Biol. 81, 389–400.
Seirin-Lee, S., Gaffney, E.A., Monk, N.A.M., 2010. The influence of gene expression time delays on Gierer–Meinhardt pattern formation systems. Bull. Math. Biol. doi:10.1007/s11538-010-9532-5.
Solnica-Krezel, L., 2003. Vertebrate development: taming the nodal waves. Curr. Biol. 13, R7–R9.
Sorkin, A., von Zastrow, M., 2002. Signal transduction and endocytosis: close encounters of many kinds. Nat. Rev. Mol. Cell Biol. 3, 600–614.
Stoscheck, C.M., Carpenter, G., 2002. Down-regulation of egf receptors: direct demonstration of receptor degradation in human fibroblasts. J. Cell Biol. 98, 1048–1053.
Tennyson, C.N., Klamut, H.J., Worton, R.G., 1995. The human dystrophin gene requires 16 hr to be transcribed and is contranscriptionally spliced. Nat. Genet. 9, 184–190.
Turing, A., 1952. The chemical basis of morphogenesis. Philos. Trans. R. Soc. Lond. B 237, 37–72.
Uriu, K., Iwasa, Y., 2007. Turing pattern formation with two kinds of cells and a diffusive chemical. Bull. Math. Biol. 67, 2515–2536.
Varea, C., Aragon, J., Barrio, R., 1997. Confined Turing patterns in growing systems. Phys. Rev. E 56(1), 1250–1253.
Wells, A., Welsh, J.B., Lazar, C.S., Wiley, H.S., Gill, G.N., Rosenfeld, M.G., 1990. Ligand-induced transformation by a noninternalizing epidermal growth factor receptor. Science 247, 962–964.
Zeng, W., Thomas, G., Glazier, J., 2004. Non-Turing stripes and spots: a novel mechanism for biological cell clustering. Physica A 341, 482–494.